

# Development of a Time Projection Chamber Using Gas Electron Multipliers (GEM-TPC)

Susumu Oda, Hideki Hamagaki, Kyoichiro Ozawa, Masahide Inuzuka, Takao Sakaguchi, TadaAki Isobe, Taku Gunji, Shota Saito, Yuhei Morino, Yorito Yamaguchi, Shin'ya Sawada and Satoshi Yokkaichi

**Abstract**—A prototype of time projection chambers using gas electron multipliers (GEM-TPC) has been developed for relativistic heavy ion collision experiments. The performance of the GEM-TPC was investigated using particle beams at KEK with 3 kinds of gases (Ar(90%)-CH<sub>4</sub>(10%), Ar(70%)-C<sub>2</sub>H<sub>6</sub>(30%) and CF<sub>4</sub>). Detection efficiency of 99%, spatial resolution of 80  $\mu$ m in the pad-row direction and double track resolution of 12 mm in the drift direction were achieved. The test results show that the GEM-TPC meets requirements of relativistic heavy ion collision experiments. This paper describes the configuration and performance of the GEM-TPC.

**Index Terms**—Time projection chamber, gas electron multiplier.

## I. INTRODUCTION

RELATIVISTIC heavy ion collision experiments are performed to study hadronic matter under high temperature and high density condition. Central tracking detectors of the relativistic heavy ion collision experiments have special difficulties due to high particle multiplicity and high event rates. In  $\sqrt{s_{NN}} = 200$  GeV Au+Au collisions at the Relativistic Heavy Ion Collider (RHIC) at Brookhaven National Laboratory, the average charged particle multiplicity  $\langle dN_{ch}/d\eta|_{\eta=0} \rangle$  is 170 [1]. Under this condition, the average charged particle density is 0.03 cm<sup>-2</sup> and the charged particle rate is  $\sim 300$  cps/cm<sup>2</sup> at a point 30 cm away from the vertex.

Since a relatively low transverse momentum range ( $p_T \sim 0.2$ –20 GeV/c) is required to be covered for the study of relativistic heavy ion collision, the magnetic field should be kept low ( $\sim 1$  T). However, high momentum resolution of  $\delta p_T/p_T^2 \sim 10^{-3}$  (GeV/c)<sup>-1</sup> is desired in future experiments, e.g., to resolve the  $\Upsilon$  states at RHIC-II [2]. To achieve such good resolution with a magnetic field of 1 T and a 1-m radius solenoidal tracker, spatial resolution of 200  $\mu$ m is needed. High double track resolution of  $\sim 1$  cm is also required to cope with the high particle multiplicity.

The double track resolution of ordinary wire chambers is limited by the space of wires and it is difficult to satisfy the

S.X. Oda, H. Hamagaki, K. Ozawa, M. Inuzuka, T. Sakaguchi, T. Isobe, T. Gunji, S. Saito and Y. Morino are with Center for Nuclear Study, Graduate School of Science, University of Tokyo, Tokyo, Japan (e-mail: oda@cns.s.u-tokyo.ac.jp).

Y.L. Yamaguchi is with Waseda University, Advanced Research Institute for Science and Engineering, Tokyo, Japan.

S. Sawada is with KEK, High Energy Accelerator Research Organization, Tsukuba-shi, Japan.

S. Yokkaichi is with RIKEN (The Institute of Physical and Chemical Research), Wako, Japan.

above requirements. A TPC using micro-pattern gas detectors (MPGD), such as gas electron multipliers (GEM) [3], for signal amplification is a strong candidate for the central tracking detector because the novel structure of MPGD may achieve both excellent spatial resolution and high rate capability with a low amount of material [4], [5].

## II. GEM-TPC PROTOTYPE

### A. Mechanical Structure

A GEM-TPC prototype, which consists of an end cap chamber, a field cage and a gas vessel, was developed. Figure 1 shows the endcap and the field cage. The field cage is a cuboid with dimensions of  $36 \times 17 \times 17$  cm<sup>3</sup>. Either a triple GEM (the effective area is  $10 \times 10$  cm<sup>2</sup>) or an MWPC is used for the end cap chamber on readout pads. The triple GEM made by CERN was used for the measurement. The gap between two GEMs was 2 mm and the gap between the bottom GEM and pads was 1.5 mm. Two kinds of readout pads with different

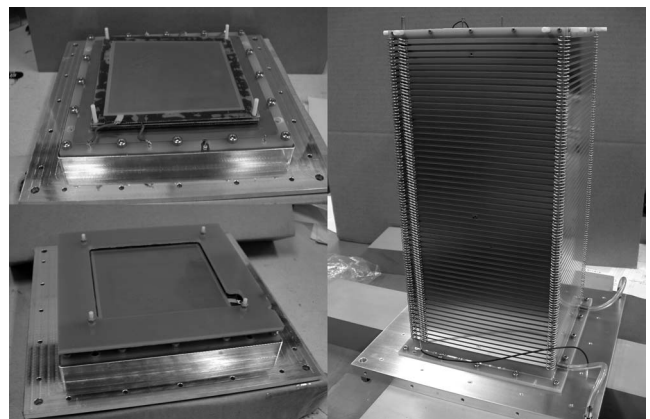


Fig. 1. The end cap without the end plate (top left), with the end plate (bottom left) and the field cage (right).

shapes, rectangle and chevron (zigzag), were made in order to study the dependence of the spatial resolution on shapes (see Fig. 2). Since chevron pads may increase the number of hit pads by charge sharing, chevron pad is expected to have better spatial resolution than rectangular one. Both kinds of pads, which are made of gold-plated copper, have the same area of  $1.09 \times 12.0$  mm<sup>2</sup>. Relatively narrow width pads are required for charge sharing with small diffusion gas, such as CF<sub>4</sub>. The field cage consists of 115 gold-plated copper strips connected

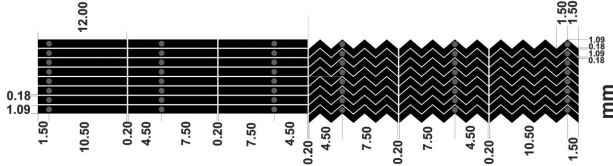


Fig. 2. Readout pad layout. Each pad has an area of  $1.09 \times 12.0 \text{ mm}^2$ .

TABLE I  
PROPERTIES OF THE 3 KINDS OF GASES

Gas	Ar(90%) -CH <sub>4</sub> (10%)	Ar(70%) -C <sub>2</sub> H <sub>6</sub> (30%)	CF <sub>4</sub>
Operated electric field (V/cm)	130	390	570
Drift velocity (cm/ $\mu$ s)	5.48	5.01	8.90
Transverse diffusion ( $\mu$ m/ $\sqrt{\text{cm}}$ )	570	306	104
Longitudinal diffusion ( $\mu$ m/ $\sqrt{\text{cm}}$ )	378	195	82
Mean energy for ion-electron pair production (eV)	26	26	54

with 1-M $\Omega$  resistors in series on FR4 boards and creates a uniform electric field. At the end of the resistor chain, additional resistors are placed to adjust the voltage of the bottom of the field cage to the surface voltage of the top GEM. The electric field uniformity is  $\int_0^{30 \text{ cm}} (E_{\perp}/E) dz \leq 1 \text{ mm}$  in the GEM effective area of  $10 \times 10 \text{ cm}^2$ .

### B. Front End Electronics

A charge sensitive preamplifier consisting of two kinds of operational amplifiers (AD8058 and AD8132, Analog Devices, Inc.) was developed for the GEM-TPC. Its time constant is  $\tau = 1 \text{ } \mu\text{s}$  and its effective gain is  $G = 3.2 \text{ V/pC}$ . This gain was determined to match the expected signal amplitude with the dynamic range ( $0 \sim -1 \text{ V}$ ) of a flash ADC (FADC) module (RPV-160, REPIC Co., Ltd.). The resolution and the sampling rate of the FADC is 8 bits and 100 MHz, respectively. The signals are transmitted from the preamplifiers to the FADCs through 8-m shielded twisted cables.

### C. Gas

Three kinds of gases, a gas mixture of Argon(90%)-CH<sub>4</sub>(10%) (commonly called P10), a gas mixture of Argon(70%)-C<sub>2</sub>H<sub>6</sub>(30%) and pure CF<sub>4</sub>(99.999%), were used to investigate the performance of the GEM-TPC with different gas properties. Properties of these gases are shown in Table I. Drift velocity and diffusion coefficient were calculated by Magboltz [6]. Characteristics of each gas are as follows. Ar(90%)-CH<sub>4</sub>(10%) is widely used in TPC and GEM. A fast

drift velocity which peaks at a low electric field of 130 V/cm is the primary attribute of Ar-CH<sub>4</sub>. Such a low electric field is an advantage for detector operation. However, its diffusion coefficients are large. Ar(70%)-C<sub>2</sub>H<sub>6</sub>(30%) is a popular chamber gas, but there are few results with GEM. Although its diffusion coefficients are smaller than that of Ar-CH<sub>4</sub>, the drift velocity peaks at a relatively high electric field of 550 V/cm. CF<sub>4</sub> gas is widely being studied as TPC and GEM gas because of its very small diffusion coefficients and its very fast drift velocity. These properties of CF<sub>4</sub> will be advantages in high particle multiplicity condition of relativistic heavy ion collision experiments. The drift velocity of CF<sub>4</sub> does not saturate. A high electric field is needed for detector operation with CF<sub>4</sub>.

Gas flow rate is set at  $\sim 200 \text{ ml/min}$  using a mass flow controller (SEC-E40, ESTEC Co., Ltd.). Gas pressure is also set at atmospheric pressure using a bubbler filled with silicone oil.

1) *Gain Measurement:* Effective gas gains were measured using an <sup>55</sup>Fe X-ray (5.9 keV) source. X-ray creates primary electrons by photoelectric effect with a gas molecule. The

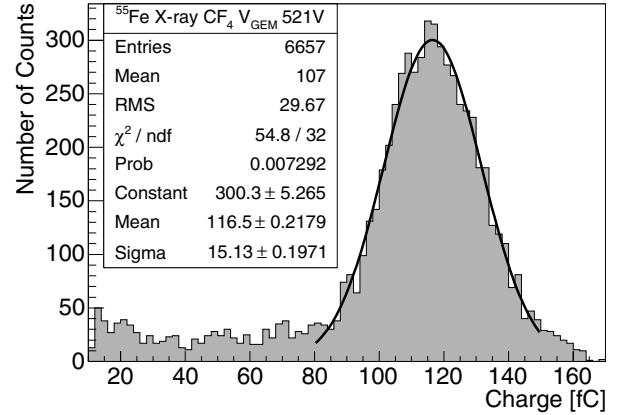


Fig. 3. Measured <sup>55</sup>Fe X-ray (5.9 keV) charge spectrum with CF<sub>4</sub>. The energy resolution is  $\sigma_E/E = 13\%$ .

obtained <sup>55</sup>Fe X-ray spectrum with CF<sub>4</sub> is shown in Fig. 3. The gain curves of the 3 kinds of gases are shown in Fig. 4 and the gain of  $10^4$  was achieved with each gas. The energy resolution ( $\sigma_E/E$ ) with Ar-CH<sub>4</sub>, Ar-C<sub>2</sub>H<sub>6</sub> and CF<sub>4</sub> is 11%, 10% and 13%, respectively. The energy resolution of 13 % with CF<sub>4</sub> using <sup>55</sup>Fe X-ray is comparable with the resolution obtained by other group (16%) [7].

### III. PERFORMANCE TEST

In order to evaluate the basic performance of the GEM-TPC, a beam test was conducted at  $\pi 2$  test beam line of the 12-GeV Proton Synchrotron at KEK (KEK-PS) in Japan. Evaluation items of the GEM-TPC were detection efficiency, spatial resolution in the pad-row direction and the drift direction, particle identification capability using  $dE/dx$  and double track resolution. Their dependence on gas (Ar(90%)-CH<sub>4</sub>(10%), Ar(70%)-C<sub>2</sub>H<sub>6</sub>(30%) and CF<sub>4</sub>), drift length (20–290 mm), readout pad shape (rectangle and chevron), beam

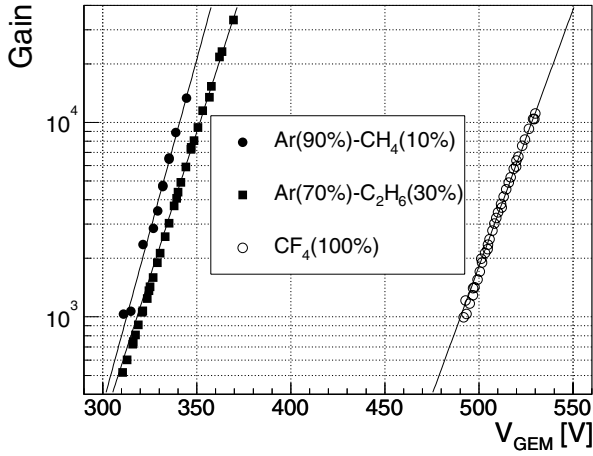


Fig. 4. Measured gain curves with the 3 kinds of gases (Ar(90%)-CH<sub>4</sub>(10%), Ar(70%)-C<sub>2</sub>H<sub>6</sub>(30%) and CF<sub>4</sub>) as functions of the voltage across the GEMs,  $V_{GEM}$ .

momentum (0.5–3.0 GeV/c) and gain of GEM ( $7 \times 10^2$ – $2 \times 10^4$ ) was also evaluated.

Figure 5 shows a schematic view of the detector setup. Three

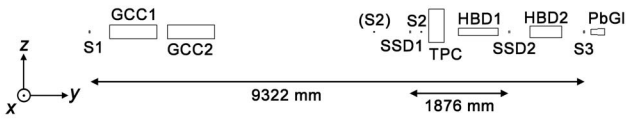


Fig. 5. Schematic view of the detector setup in the performance test.

scintillation counters (S1, S2 and S3) were used for triggering and time of flight measurement. Two gas Cherenkov counters (GCC1 and GCC2) filled with 2.5-atm CO<sub>2</sub> gas were used for electron identification. Two silicon strips detectors (SSD1 and SSD2) were used for particle tracking. Two hadron blind detectors (HBD1 and HBD2) were tested at the same time and the results are shown in [8]. No magnetic field was applied to the GEM-TPC.

Figure 6 shows a typical GEM-TPC signal with Ar-C<sub>2</sub>H<sub>6</sub>. To evaluate the pulse height and time zero (arrival time), the following function is fitted to the FADC spectrum,

$$ADC(t) = p_0 + \frac{p_1 \cdot \exp(-(t - p_2)/p_3)}{1 + \exp(-(t - p_2)/p_4)}, \quad (1)$$

where  $t$  is time. The fitting parameters in the above function can be recognized as follows;  $p_0$ : pedestal,  $p_1$ : pulse height,  $p_2$ : time zero,  $p_3$ : time constant,  $p_4$ : rise time. The obtained pulse height and time zero were used for hit position determination. The hit position in each pad row was determined by weighted mean of pulse heights.

#### IV. RESULTS

##### A. Detection Efficiency

Single-pad-row detection efficiency was measured as a function of a GEM gain with 3 kinds of gases and results are shown

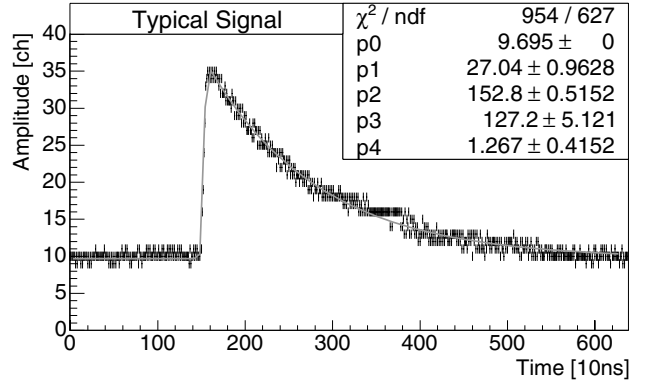


Fig. 6. A typical GEM-TPC signal created by a 1-GeV/c electron beam. The drift gas is Ar(70%)-C<sub>2</sub>H<sub>6</sub>(30%), the drift length is 85 mm and the pad shape is chevron. A voltage across GEM is  $V_{GEM} = 341$  V.

in Fig. 7. In this measurement, the drift length of 20 mm for Ar-CH<sub>4</sub>, and 85 mm for Ar-C<sub>2</sub>H<sub>6</sub> and CF<sub>4</sub> was used. The efficiency reaches 99% at the plateaus.

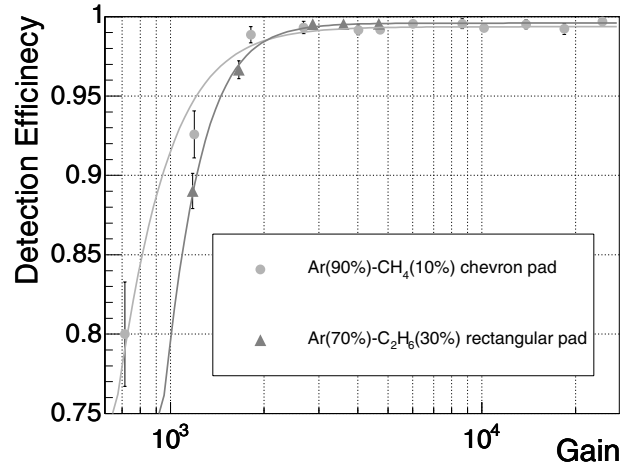


Fig. 7. Detection efficiency of the GEM-TPC as a function of a GEM gain.

##### B. Transverse Diffusion Coefficient

Transverse diffusion coefficients were measured using spatial distribution of secondary electrons in the pad-row direction. The distribution can be represented by Gaussian distribution. The Gaussian sigma of the pad response function,  $s_x$ , behaves  $s_x^2(L) = s_{x0}^2 + C_{DT}^2 \cdot L$ , where  $L$  is the drift length,  $C_{DT}$  is the transverse diffusion coefficient and  $s_{x0}$  is the width of the induced charge distribution, which depends on the configuration of the readout system.  $s_{x0}^2$  is shown in Fig. 8 as a function of the drift length. The measured  $s_{x0}$  and  $C_{DT}$  are shown in Table II. The measured values of  $C_{DT}$  agree well with the calculated values of  $C_{DT}$  shown in Table I.

##### C. Spatial Resolution

Single-pad-row spatial resolution in the pad-row direction and the drift direction was evaluated for the drift length of 20–

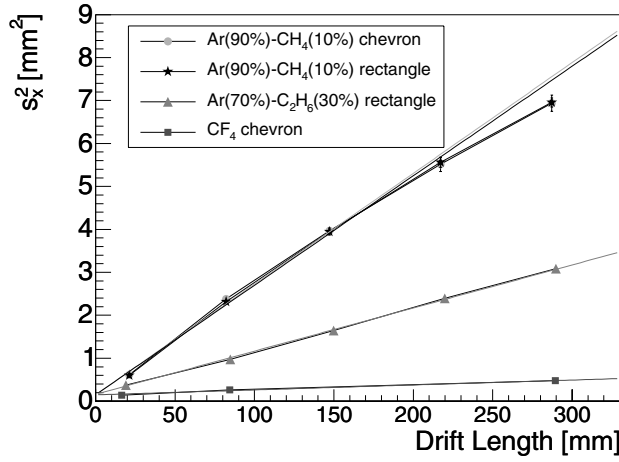


Fig. 8. The squared width of the diffused secondary electrons  $s_x^2$  for the 3 kinds of gases.

TABLE II  
THE MEASURED WIDTH OF INDUCED CHARGE DISTRIBUTION AND THE TRANSVERSE COEFFICIENTS

Gas Pad shape	$s_{x0}$ ( $\mu\text{m}$ )	$C_{DT}$ ( $\mu\text{m}/\sqrt{\text{cm}}$ )
Ar(90%)-CH <sub>4</sub> (10%) chevron	$385 \pm 101$	$508 \pm 7$
rectangle	$387 \pm 101$	$505 \pm 7$
Ar(70%)-C <sub>2</sub> H <sub>6</sub> (30%) rectangle	$402 \pm 43$	$317 \pm 4$
CF <sub>4</sub> chevron	$383 \pm 37$	$107 \pm 6$

290 mm. The single-pad-row spatial resolution was evaluated using the hit positions of three adjacent pad rows. The measured spatial resolution is shown in Fig. 9. The best resolution is 79  $\mu\text{m}$  in the pad-row direction and 313  $\mu\text{m}$  in the drift direction and it was obtained with Ar-C<sub>2</sub>H<sub>6</sub> gas and rectangular pads at 13-mm drift. Spatial resolution is similar between the two kinds of pads.

The spatial resolution depends on the drift length of  $L$ . This dependence can naively be understood as  $\sigma_x^2(L) = \sigma_{x0}^2 + C_{DT}^2 \cdot L/N_{eff}$ , where  $N_{eff}$  is the effective number of secondary electrons and  $\sigma_{x0}$  is extrapolated resolution without drift [5]. The number of secondary electrons,  $N$ , and the measured number of effective secondary electrons,  $N_{eff}$ , of 1-GeV/c  $\pi^-$  beam for track length of 12 mm are shown in Table III. A small fraction of secondary electrons contribute to spatial resolution.

#### D. Particle Identification Capability

Particle identification capability was studied with positrons, muons, pions, protons and deuterons by measuring pulse heights. The beam momentum range was 0.5–3.0 GeV/c. Figure 10 shows the measured mean energy loss for the 5

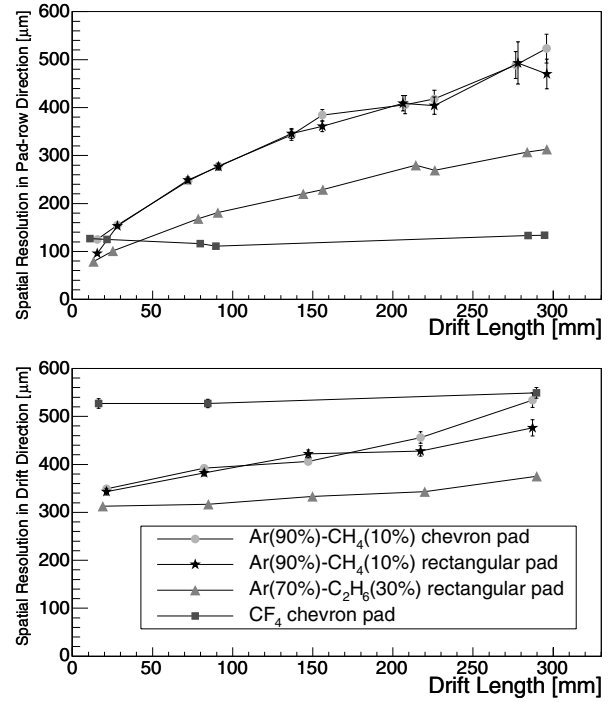


Fig. 9. Spatial resolution in the pad-row direction (top) and the drift direction (bottom).

TABLE III  
THE NUMBER OF EFFECTIVE SECONDARY ELECTRONS.

Gas Pad shape	$N_{eff}$	$N$	$N_{eff}/N$
Ar(90%)-CH <sub>4</sub> (10%) chevron	$31 \pm 1$	119	$0.26 \pm 0.01$
rectangle	$30 \pm 1$	119	$0.25 \pm 0.01$
Ar(70%)-C <sub>2</sub> H <sub>6</sub> (30%) rectangle	$31 \pm 1$	131	$0.23 \pm 0.01$
CF <sub>4</sub> chevron	$86 \pm 23$	147	$0.58 \pm 0.15$

kinds of particle species. Curves of expected energy losses are also shown in Fig. 10. The Berger-Seltzer formula for positron and the Bethe-Bloch formula for the other particles with density effect correction and the shell correction were used for calculation.

In order to estimate the particle identification capability of a large GEM-TPC, a Monte-Carlo simulation was performed using measured energy loss spectra for 1-GeV/c pion and proton. To improve the energy resolution, a truncated mean method was used. Energy resolution of pion will be 9% and the pion rejection factor with 99% proton efficiency is expected to be 200 with 50-cm track length.

#### E. Double Track Resolution

To evaluate double track resolution, the measured distribution of distance of two tracks in the drift direction were compared

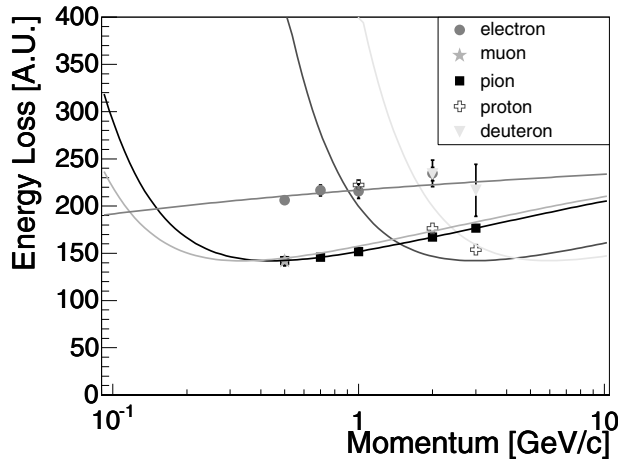


Fig. 10. Measured energy loss for 5 kinds of particle species. The curves are the expected energy losses.

with the simulated distribution. The ratio of the measured distribution to the simulated distribution is shown in Fig. 11. Two tracks with a distance of  $>12$  mm can almost be distinguished.

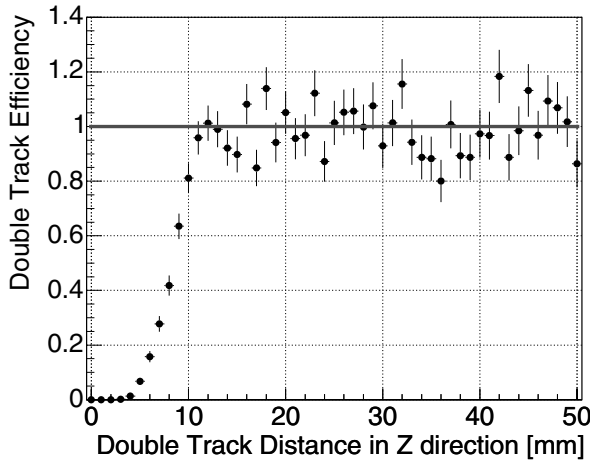


Fig. 11. Double track detection efficiency in the drift direction.

#### F. Beam Rate Dependence

One of the advantages of GEM-TPC is ion feedback suppression. The effect of the ion feedback on the GEM-TPC performance was studied by measuring beam rate dependence of detection efficiency and spatial resolution (see Fig. 12). The total beam rate in the active GEM-TPC region was up to order of  $10^5$  cps. At the maximum beam rate of 4800 cps/cm<sup>2</sup>, the detection efficiency and the spatial resolution were worsened by factors of 3% and 10%, respectively. However, the results still indicate high performance of the GEM-TPC.

The beam rate exceeds the typical rates of RHIC and LHC which will be 170 cps/cm<sup>2</sup> and 1400 cps/cm<sup>2</sup>, respectively, at a point 30 cm away from the vertex.

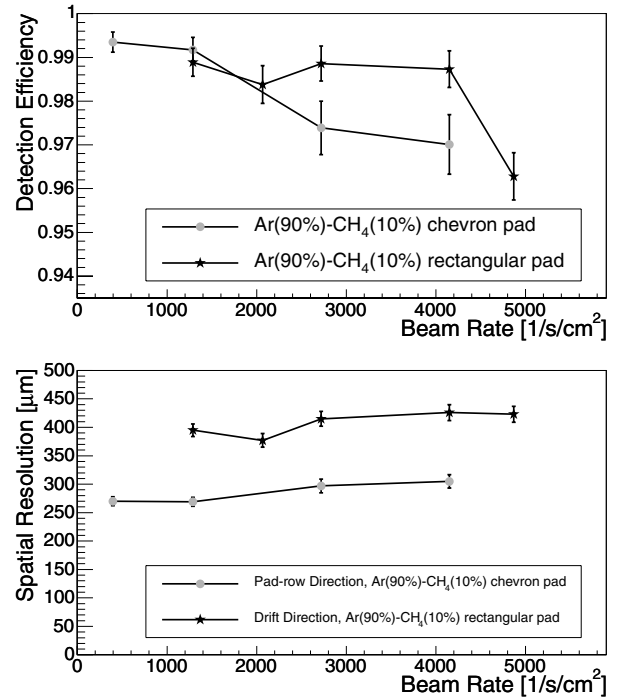


Fig. 12. Dependence of the detection efficiency (top) and the spatial resolution on the beam rate.

#### V. CONCLUSION

A GEM-TPC prototype has been constructed toward a tracker in high event rate and high particle multiplicity condition.

To evaluate the performance of the GEM-TPC, a beam test has been conducted at KEK-PS. Detection efficiency, spatial resolution, particle identification capability and double track resolution were studied. The GEM-TPC held high detection efficiency and good spatial resolution with a high particle rate of 4800 cps/cm<sup>2</sup>, which exceeds ones of RHIC and LHC.

The results indicate that the GEM-TPC meets the requirements for central tracking detectors in the next generation of relativistic heavy ion collision experiments.

#### ACKNOWLEDGMENT

The authors would like to thank KEK-PS group, especially Dr. M. Ieiri, for their good service of the accelerator and kind cooperation. The authors are thankful to staff and students of the Weizmann Institute of Science, Hiroshima University and University of Tsukuba for their cooperation in the performance test.

#### REFERENCES

- [1] B.B. Back *et al.*, Phys. Rev. **C 65** (2002) 031901.
- [2] P. Steinberg *et al.*, nucl-ex/0503002.
- [3] F. Sauli, Nucl. Instr. and Meth. **A 386** (1997) 531.
- [4] J. Kaminski *et al.*, Nucl. Instr. and Meth. **A 535** (2004) 201.
- [5] R.K. Carnegie *et al.*, Nucl. Instr. and Meth. **A 538** (2005) 372.
- [6] S.F. Biagi, Nucl. Instr. and Meth. **A 421** (1999) 234.
- [7] A. Kozlov *et al.*, Nucl. Instr. and Meth. **A 523** (2004) 345.
- [8] Z. Fraenkel *et al.*, Nucl. Instr. and Meth. **A 546** (2005) 466.